Journal of Solid State Chemistry 266 (2018) 70–73

Contents lists available at ScienceDirect

Journal of Solid State Chemistry

journal homepage: www.elsevier.com/locate/jssc

A Zn based anionic metal-organic framework for trace Hg^{2+} ion detection

Yating Wan, Danna Zou, Yuanjing Cui*, Yu Yang, Guodong Qian*

State Key Laboratory of Silicon Materials, Cyrus Tang Center for Sensor Materials and Applications, School of Materials Science and Engineering, Zhejiang University, Hangzhou 310027, China

ARTICLE INFO

Keywords:
Ionic metal-organic framework
Luminescent
Trace Hg^{2+} ions
Sensing

ABSTRACT

As one of the most toxic heavy metal ions, Hg^{2+} exists widely in the living surroundings of human beings and excessive Hg^{2+} possesses a great threat to human health. The maximum allowable concentration of Hg^{2+} in drinking water is only 10 nM (2 ppb) by U.S. EPA standard. Ionic metal-organic framework (iMOF) is considered in view of high sensitive, anti-interferential material for Hg^{2+} detection still remain a challenge. Herein we designed and synthesized a novel Zn based anionic MOF **Zn-TPTC**, which was characterized by single crystal diffraction and other method. Its performance on Hg^{2+} (10^{-6}–10^{-4} M) detection were studied and the detection limit (LOD) is calculated as low as 3.67 nM. Interference experiments showed that **Zn-TPTC** could exclude the interference of other ions, which could be attributed to the effective pore size, anionic framework and multiple N sites in ligand, providing us new ideas for the selection and design of MOF for detection application.

1. Introduction

Mercury is a kind of extremely toxic and dangerous contaminant which could evaporate at room temperature and spread widely in the living surroundings of human beings [1]. In addition, as a type of heavy metal ion to complete the circulation in ecosystem, it could be very easy for Hg^{2+} to enter the food chain and bioaccumulate in human body due to its non-biodegradable property [2,3]. What's worse is that even in a low concentration, Hg^{2+} ions can lead to a variety of chronic diseases like mental nerve abnormalities, gingivitis and tremor [4]. Therefore, the prevention and control of mercury poisoning has become an important issue facing all countries in the world. Mercury exist in water mainly in Hg^{2+} state and the maximum allowable level of Hg^{2+} in drinking water is only 10 nM (2 ppb) by U.S. EPA standard, which requires the designing of highly sensitive and anti-interferential probe [4,5]. Compared with the existing methods of Hg^{2+} detection such as liquid chromatography, gas chromatography, atomic absorption/fluorescence spectroscopy, fluorescence-based sensors have drawn a lot of attention because of rapid response, excellent selectivity and low cost [6–10].

Ionic luminescent metal-organic framework as a kind of charged hybrid material composed of metal atoms and organic ligand, combining the advantages of electrification and intrinsic properties of metal-organic framework (MOF), such as porous structure and easily design and synthesis, etc., possessing a great prospect of application in gas storage and separation, drug loading and controlled release, luminescence and sensing, etc. [11–23]. What is worth mentioning is that multifunctional sites in ligand from the framework could provide plenty of other functions and increase the designability of the material [24–29].

Based on the aforementioned reasons and given that Hg^{2+} has a higher affinity to nitrogen atoms, organic ligand containing multiple N atoms was chosen for designing a novel ionic luminescent MOF for trace Hg^{2+} detection. Here we designed and synthesized an novel Zn based anionic MOF, **Zn-TPTC** (TPTC = [2,2':6',2"-Terpyridine]-4,4',4"-tricarboxylic acid) and the crystal was characterized by single crystal diffraction, powder X-ray diffraction, elemental analyses, thermogravimetric analyses and infrared absorption spectrum. The performance on Hg^{2+} detection in water was tested in a range of 10^{-6}–10^{-4} M and there is a linear relationship between the emission intensity of **Zn-TPTC** and the concentration of Hg^{2+}. **Zn-TPTC** has special recognition to Hg^{2+} and as for the mechanism, the strong affinity of Hg^{2+} and N on the ligand accounts for most. The detection limit (LOD) is calculated as low as 3.67 nM which is much lower than the U.S. EPA standard of drinking water and it can be assumed that such a low detection limit is related to the pore size, multiple N sites and anionic framework.

* Corresponding author.
E-mail addresses: cuiyj@zju.edu.cn (Y. Cui), gdqian@zju.edu.cn (G. Qian).

https://doi.org/10.1016/j.jssc.2018.07.013
Received 13 June 2018; Received in revised form 10 July 2018; Accepted 12 July 2018
Available online 17 July 2018
0022-4596/

Table 1
Crystallographic Data for **Zn-TPTC**.

Compound	**Zn-TPTC**
Empirical formula	C72 H32 N12 O24 Zn5
Formula weight	1776.05
Temperature	296(2) K
Wavelength	0.71073 Å
Crystal system	Monoclinic
Space group	C 2/c
a(Å)	35.367(4)
b(Å)	26.090(2)
c(Å)	25.014(2)
α(°)	90°
β(°)	134.963(7)°
γ(°)	90°
Volume	16,332(3) $Å^3$
Z	4
Density (calculated)	0.722 Mg/m^3
F(000)	3560
Absorption coefficient	0.763 mm^{-1}
Theta range for data collection	1.127–26.071°
Reflections collected	84,029
Independent reflections	16,039 [R(int) = 0.1038]
Data / restraints / parameters	16,039 / 0 / 510
Goodness-of-fit on F2	1.009
Final R indices [I > 2sigma(I)]	R1 = 0.0570, wR2 = 0.1613
R indices (all data)	R1 = 0.1673, wR2 = 0.2182
Largest diff. peak and hole	0.648 and − 0.316 $e.Å^{-3}$

2. Experimental section

2.1. Materials and synthesis

All reagents were purchased commercially and used without further purification.

Synthesis of Zn-TPTC: 0.01 mmol (3.65 mg) [2, 2':6', 2"-Terpyridine]-4, 4', 4"-tricarboxylic acid and 0.01 mmol (2.97 mg) $Zn(NO_3)_2{\cdot}6H_2O$ were dissolved in mixed solution of DMF (2 mL) and water (2 mL). After then the mixed solution was acidized by 140 μL HNO_3 before being transferred to a 15 mL glass bottle and kept in 110 °C oven for three days. Octahedral yellow crystal were obtained after the bottle was cooling down to room temperature.

2.2. Characterization

Powder X-ray diffraction (PXRD) patterns were obtained by X'Pert PRO diffractometer with Cu-Kα (λ = 1.542 Å) radiation at room temperature. Elemental analyses (EA) for C, H and N were performed on an EA1112 microelemental analyzer. Netzsch TG209F3 was utilized for thermogravimetric analyses (TGA) with a heating rate of 10 °C•min^{-1} under N_2 atmosphere. Thermo Fisher Nicolet iS10 spectrophotometer was used to test the infrared absorption spectrum and sample was tableted with KBr in ratio of 1:20. Crystallographic measurements were taken on Oxford Xcalibur Gemini Ultra diffractometer with graphite-monochromatic Mo-Kα radiation (λ = 0.71073 Å) and an Atlas detector at 293 K. X-ray photoelectron spectroscopy (XPS, Axis Supra, Kratos Analytical Ltd) analysis was performed to determine the coordination state of N, and the binding energy data were calibrated with reference to the C 1s signal at 284.6 eV.

Quantum efficiency of the sample were obtained on Edinburgh FLF920 multi-function fluorescence spectrometer in an absolute method with xenon lamp as the excitation light source and red PMT as detector. Excitation and emission slit size were 5 nm and 0.3 nm, respectively. Photoluminescence spectroscopy (PL) including excitation and emission spectra were obtained by Hitachi F4600 steady-state fluorescence spectrometer. Excitation light source was xenon lamp with excitation and emission slit size of 2.5 nm, 2.5 nm, respectively. PMT detector's voltage was 750 V and the scanning speed was 240 nm•min^{-1}.

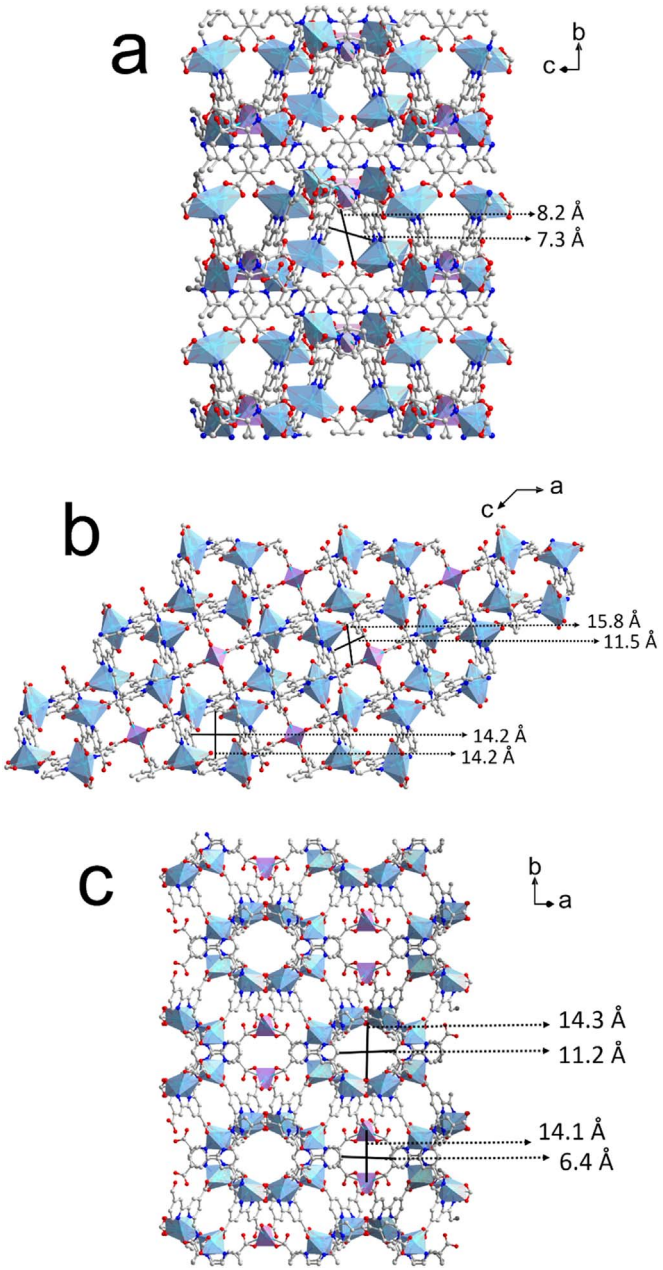

Fig. 1. The structure of **Zn-TPTC** in view of (a) a axis; (b) b axis; (c) c axis. Zn3-SBUs are represented in purple and Zn1-SBUs, Zn2-SBUs are represented in blue. Numbers represent interatomic distance without removal of the Van Der Waals radius of atoms.

3. Results and discussion

Zn-TPTC is an anionic MOF whose ligand is [2, 2': 6', 2"-Terpyridine]- 4, 4', 4"-tricarboxylic acid and metal nitrates and the ligand were mixed and reacted in-situ to obtain octahedral yellow crystal. According to single crystal diffraction result, **Zn-TPTC** crystallizes in monoclinic crystal system with space group of *C*2/*c* and the configuration of Zn centers can be classified as two groups in terms of their coordination atoms: (1) Zn3 is coordinated with four O atoms from four independent ligand; (2) Zn1 and Zn2 are coordinated with four O atoms from two independent carboxylic acids and three N atoms from another ligand (Scheme S1a, Table 1, ESI). The second building units (SBU) of Zn atoms in different types of coordination patterns are marked as separate colours (Zn1-SBU and Zn2-SBU in blue and Zn3-SBU in purple) (Fig. 1). It is worth noting that the number ratio of Zn3 to Zn1 + Zn2 is 1:4.

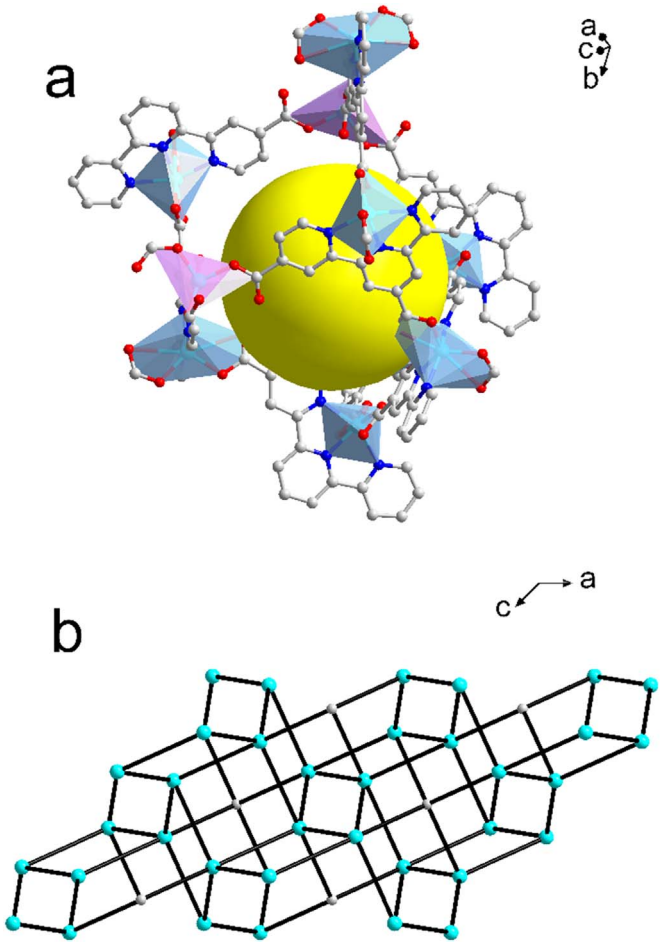

Fig. 2. (a) The largest cage in **Zn-TPTC**; (b) simplified topology of **Zn-TPTC**, blue ball represent $ZnC_{18}H_8N_3O_5$, grey ball represent ZnO_4, from b axis.

As for coordination pattern of ligand, it is much simpler for every ligand is coordinated with one Zn1 and two Zn2 and one Zn3 to form a three-dimensional structure (Scheme S1b, Table 1, ESI). It can also be explained as the two types of Zn-SBU in **Zn-TPTC** are further connected to adjacent units through the TPTC ligands, which lead to the formation of a three-dimensional anionic framework with channels along a, b, c axis with size of 8.2 × 7.3 Å^2, 14.2 × 14.2 Å^2 and 11.5 × 15.8 Å^2, 6.4 × 14.1 Å^2 and 11.2 × 14.3 Å^2, respectively (Fig. 1). There exists a relatively large pore of about 11 Å in the 3D structure of **Zn-TPTC** so it can be assumed that the pores can provided an enrichment site for detection (Fig. 2a). Topology of **Zn-TPTC** is analysed for further simplifying the crystal structure (Fig. 2b). The blue balls represent $ZnC_{18}H_8N_3O_5$ and the grey ball represents ZnO_4.

Element analysis shows that the structure of **Zn-TPTC** is $Zn_5TPTC_4((CH_3)_2NH_2)_2{\bullet}DMF_3{\cdot}(H_2O)_{24}$. The $(CH_3)_2NH_2^+$ was introduced in the channels of framework to balance the valence states. The phase purity of **Zn-TPTC** was confirmed by powder X-ray diffraction (PXRD) (Fig. S1, ESI) and thermogravimetric analysis (TGA) (Fig. S2, ESI). The PXRD patterns of the synthesized **Zn-TPTC** are consistent with that of simulated by single crystal diffraction and **Zn-TPTC** shows excellent thermal stability with high framework decomposition temperature (350 °C), which also enlarges its application range. Infrared spectra shows the absorption peak of carboxylic acid in ligand changed from 1710 cm^{-1} to 1622 cm^{-1} in **Zn-TPTC**, verifying that coordination between ligand and metal exist and MOF material are formed (Fig. S3, ESI).

The fluorescent properties of **Zn-TPTC** were studied and the fluorescence of **Zn-TPTC** is from the ligand. MOF in water exhibits the same fluorescence as that in solid state (Fig. S4, ESI). It is worth

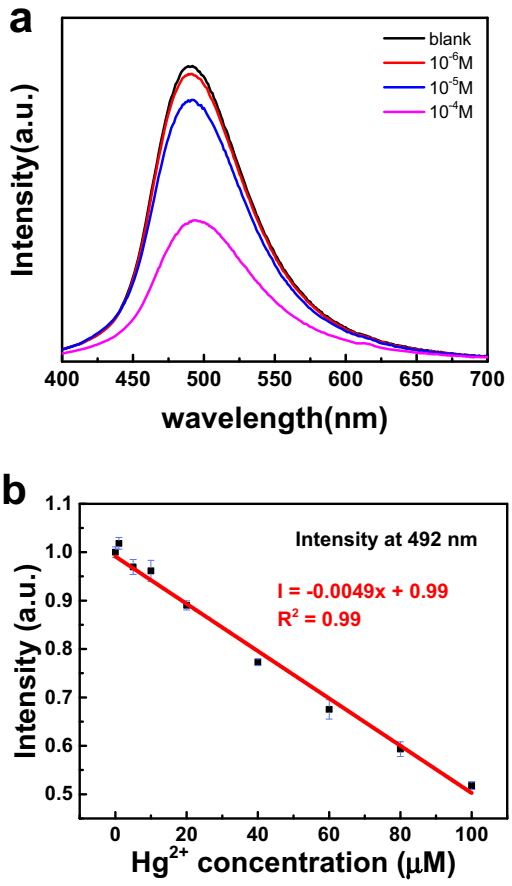

Fig. 3. (a) the emission spectrum of **Zn-TPTC** (1 mg) in water solution (2 mL) of Hg at different concentration; (b) fitting line of maximum intensity of emission spectrum of **Zn-TPTC** (at 492 nm) and concentration of Hg ion water solution.

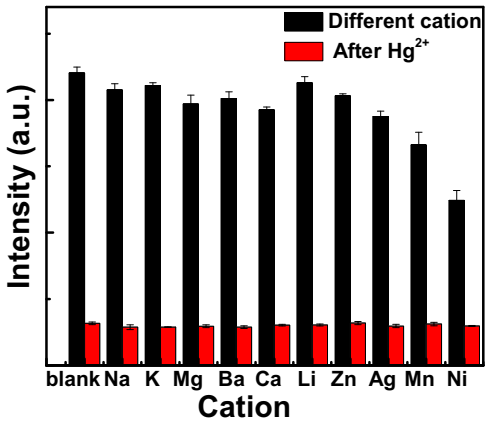

Fig. 4. Emission spectrum intensity of **Zn-TPTC** (1 mg) at 492 nm in different metal ion water solution (2 mL, 10^{-4} M) and the intensity at 492 nm after adding 10^{-4} M Hg^{2+}.

noting that the quantum efficiency of **Zn-TPTC** is greatly improved compared to pure ligand and MOF in water shows better fluorescent efficiency (Table S1, ESI). Based on the above reasons, **Zn-TPTC** water solution was chosen for Hg^{2+} detection. **Zn-TPTC** water solution was excited by 370 nm and emitted bright blue light at 492 nm. With the addition of Hg^{2+} from 10^{-6}-10^{-4} M, the fluorescent intensity gradually decreases (Fig. 2a) and there is a linear relationship between the fluorescent intensity of **Zn-TPTC** at 492 nm and the concentration of Hg^{2+} (Fig. 2b), which can be expressed as follows:

$$I = -0.0049 \times + 0.99 \quad (1)$$

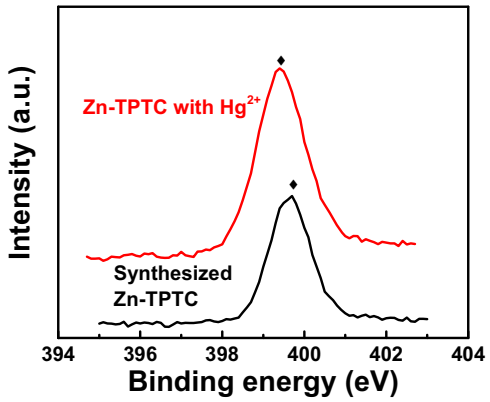

Fig. 5. Nitrogen element (1s) X-ray photoelectron spectroscopy (XPS) analysis of synthesized **Zn-TPTC** and **Zn-TPTC** immersed in Hg^{2+} water solution (10^{-4} M) for one hour.

I is the fluorescent intensity of **Zn-TPTC** at 492 nm and *x* is the concentration of Hg^{2+}. Combined with the stability of the spectrometer performance, the detection limit (LOD) is calculated as 3.67 nM, which is much lower than the EPA standard of drinking water in the United States (10 nM). This result also shows that the material can be applied to the detection of Hg^{2+} in drinking water.

In order to further verify that **Zn-TPTC** can be applied to Hg^{2+} detection in real environment, interference experiments were conducted (Fig. 3). A series of possible cations in real water samples were selected and mixed into **Zn-TPTC** water solution (10^{-4} M), and the fluorescence at 370 nm excitation were collected and normalized. It was found that the fluorescent intensity basically remain unchanged compared to pure **Zn-TPTC**. After that 10^{-4} M Hg^{2+} was added in the mixed solution and the fluorescent intensity decreased rapidly, indicating that **Zn-TPTC** could exclude the interference of other ions and detect Hg^{2+} specifically and effectively.

X-ray photoelectron spectroscopy (XPS) experiments were conducted to verify the strong affinity between Hg^{2+} and N in order to illustrate the detection mechanism. As shown in Fig. 4, Nitrogen element (1s) was chosen for explaining the difference between the synthesized sample and sample immersed in Hg^{2+} water solution. Compared with synthesized **Zn-TPTC**, the binding energy of sample treated with Hg^{2+} has a blue shift of 0.3 eV, which implies that some of N atoms of the ligand in MOF have affinity interactions with Hg^{2+} and then influence the fluorescence of MOF. This mechanism is also consistent with those reported in some literatures but we have proved this by real experiments [30–32]. Through the above experiments and previous experience, we conclude that ligand containing multiple N atoms can greatly improve the detection limit and the anionic framework may increase the attraction to cations and the pores may provide an enrichment site for Hg^{2+}, which are all supportive to lower the detection limit and also provide us new ideas for the selection and design of ligands for detection application. Fig. 5

4. Conclusions

In conclusion, a novel Zn based anionic metal-organic framework **Zn-TPTC** was designed and synthesized for the detection of trace Hg^{2+} in water. The structure and basic properties of **Zn-TPTC** were characterized and the performance on Hg^{2+} detection in a range of 10^{-6}-10^{-4} M were studied. There is a linear relationship between the fluorescent intensity of **Zn-TPTC** at 492 nm and the concentration of Hg^{2+}, and the LOD was calculated as 3.67 nM, which is much lower than the U.S. EPA standard of drinking water (10 nM). Additionally, **Zn-TPTC** could exclude the interference of other ions and detect Hg^{2+} specifically and effectively. Summing up the previous experience and our experimental results, it can be summarized that such an excellent Hg^{2+} detection effect can be attributed to pore size, anionic framework and multiple N sites in ligand, which provide us general method for the selection and design of MOF for detection application.

Acknowledgment

This work was supported by the National Natural Science Foundation of China (Nos. 51472217, 51432001, 51632008, 51772268, U1609219 and 61721005).

Appendix A. Supporting information

Supplementary data associated with this article can be found in the online version at http://dx.doi.org/10.1016/j.jssc.2018.07.013.

References

[1] D.P. Krabbenhoft, E.M. Sunderland, Science 341 (2013) 1457–1458.
[2] Q. Wang, D. Kim, D.D. Dionysiou, G.A. Sorial, D. Timberlake, Environ. Pollut. 131 (2004) 323–336.
[3] M. McNutt, Science 341 (2013) 1430.
[4] S.-R. Zhang, W. Wang, G.-J. Xu, C. Yao, Y.-H. Xu, Z.-M. Su, Inorg. Chem. Commun. 89 (2018) 73–77.
[5] S.A.A. Razavi, M.Y. Masoomi, A. Morsali, Inorg. Chem. 56 (2017) 9646–9652.
[6] L.-L. Wu, Z. Wang, S.-N. Zhao, X. Meng, X.-Z. Song, J. Feng, S.-Y. Song, H.-J. Zhang, Chem. Eur. J. 22 (2016) 477–480.
[7] Y.-Min Zhu, C.-H. Zeng, T.-S. Chu, H.-M. Wang, Y.-Y. Yang, Y.-X. Tong, C.-Y. Sua, W.-T. Wong, J. Mater. Chem. A 1 (2013) 11312–11319.
[8] S.-Y. Ding, M. Dong, Y.-W. Wang, Y.-T. Chen, H.-Z. Wang, C.-Y. Su, W. Wang, J. Am. Chem. Soc. 138 (2016) 3031–3037.
[9] W. Ma, M. Sun, L. Xu, L. Wang, H. Kuang, C. Xu, Chem. Commun. 49 (2013) 4989–4991.
[10] H. Xu, J. Gao, X. Qian, J. Wang, H. He, Y. Cui, Y. Yang, Z. Wang, G. Qian, J. Mater. Chem. A 4 (2016) 10900–10905.
[11] Y. Wan, Y. Cui, Y. Yang, G. Qian, Microporous Mesoporous Mater. 268 (2018) 202–206.
[12] A. Karmakar, A.V. Desai, Sujit K. Ghosh, Coord. Chem. Rev. 307 (2016) 313–341.
[13] H.-C. Zhou, J.R. Long, O.M. Yaghi, Chem. Rev. 112 (2012) 673–674.
[14] H. Furukawa, K.E. Cordova, M. O'Keeffe, O.M. Yaghi, Science 341 (2013) 1230444.
[15] G. Férey, C. Serre, Chem. Soc. Rev. 38 (2009) 1380–1399.
[16] M. Eddaoudi, J. Kim, N. Rosi, D. Vodak, J. Wachter, M. O'Keeffe, O.M. Yaghi, Science 295 (2002) 469–472.
[17] J. Cong, H. Xu, M. Lu, Y. Wu, Y. Li, P. He, J. Gao, J. Yao, S. Xu, Chem. Asian J. 13 (2018) 1485–1491.
[18] W. Ren, J. Gao, C. Lei, Y. Xie, Y. Cai, Q. Ni, J. Yao, Chem. Eng. J. 349 (2018) 766–774.
[19] H.-S. Lu, L. Bai, W.-W. Xiong, P. Li, J. Ding, G. Zhang, T. Wu, Y. Zhao, J.-M. Lee, Y. Yang, B. Geng, Q. Zhang, Inorg. Chem. 53 (2014) 8529–8537.
[20] J. Gao, K. Ye, L. Yang, W.-W. Xiong, L. Ye, Y. Wang, Q. Zhang, Inorg. Chem. 53 (2014) 691–693.
[21] J. Zhao, Y. Wang, W. Dong, Y. Wu, D. Li, B. Liu, Q. Zhang, ChemComm 51 (2015) 9479–9482.
[22] X.-Q. Wu, J. Zhao, Y.-P. Wu, W.-w. Dong, D.-S. Li, J.-R. Li, Q. Zhang, ACS Appl. Mater. Interfaces 10 (2018) 12740–12749.
[23] G.-W. Xu, Y.-P. Wu, W.-W. Dong, J. Zhao, X.-Q. Wu, D.-S. Li, Q. Zhang, Small 13 (2017) 1602996.
[24] B.-H. Liu, D.-X. Liu, K.-Q. Yang, S.-J. Dong, W. Li, Y.-J. Wang, Inorg. Chem. Commun. 90 (2018) 61–64.
[25] F. Xu, L. Kou, J. Jia, X. Hou, Z. Long, S. Wang, Anal. Chim. Acta 804 (2013) 240–245.
[26] C.-Y. Gao, H.-R. Tian, J. Ai, L.-J. Li, S. Dang, Y.-Q. Lan, Z.-M. Sun, Chem. Commun. 52 (2016) 11147–11150.
[27] Y. Dong, H. Zhang, F. Lei, M. Liang, X. Qian, P. Shen, H. Xu, Z. Chen, J. Gao, J. Yao, J. Solid State Chem. 245 (2017) 160–163.
[28] H. Xu, Y. Dong, Y. Wu, W. Ren, T. Zhao, S. Wang, J. Gao, J. Solid State Chem. 258 (2018) 441–446.
[29] J. Zhao, Y.-N. Wang, W.-W. Dong, Y.-P. Wu, D.-S. Li, Q.-C. Zhang, Inorg. Chem. 55 (2016) 3265–3271.
[30] A. Tadjarodi, A. Abbaszadeh, Microchim. Acta 183 (2016) 1391–1399.
[31] P. Wu, Y. Liu, Y. Liu, J. Wang, Y. Li, W. Liu, J. Wang, Inorg. Chem. 54 (2015) 11046–11048.
[32] S. Halder, J. Mondal, J. Ortega-Castro, A. Frontera, P. Roy, Dalton Trans. 46 (2017) 1943–1950.